

Synthesis and Comparison of the Optical Properties of Platinum(II) Poly-ynes with Fused and Non-Fused Oligothiophenes

Lekshmi Sudha Devi,^{†,‡} Mohammed K. Al-Suti,[§] Ning Zhang,[†] Simon J. Teat,^{||} Louise Male,[⊥] Hazel A. Sparkes,[⊥] Paul R. Raithby,^{*,⊥} Muhammad S. Khan,^{*,§} and Anna Köhler^{*,†,‡}

Cavendish Laboratory, University of Cambridge, Cambridge CB3 0HE, U.K., Department of Physics, University of Bayreuth, Bayreuth 95440, Germany, Department of Chemistry, College of Science, Sultan Qaboos University, Sultanate of Oman, The STFC Daresbury Laboratory, Daresbury, Warrington WA4 4AD, U.K., and Department of Chemistry, University of Bath, Bath BA2 7AY, U.K.

Received October 24, 2008; Revised Manuscript Received December 1, 2008

ABSTRACT: The synthesis and characterization of the thieno[3,2-*b*]thiophene and dithieno[3,2-*b*:2',3'-*d*]thiophene containing platinum(II) poly-ynes and their molecular precursors is described and the electronic structure is established by absorption, luminescence and photoinduced absorption measurements. A comparison of the electronic structure of the fused and the nonfused oligothiophenes, thieno[3,2-*b*]thiophene, dithieno[3,2-*b*:2',3'-*d*]thiophene, 2,2'-bithiophene, and 2,2':5',2''-terthiophene incorporated in platinum(II) poly-ynes is reported. We find the singlet S_1 and triplet T_1 and T_n excited states to be at higher energy in thin films made from the fused systems than from the nonfused systems. For ligands with the same number of rings, we attribute this to the decreased number of double bonds in the fused system and to the presence of an additional sulfur atom in spacers with the same number of double bonds.

I. Introduction

Oligothiophenes and polythiophenes have sparked particular interest within the area of optoelectronic materials because of their applications in organic thin film transistors and photovoltaic cells.^{1–5} Though thiophenes are known for their excellent charge transport properties, the possible disruption of conjugation caused by torsion about the single bonds and unfavorable molecular packing can be limiting factors of charge carrier mobility. It has been suggested by Zhang et al. that oligothiophenes with fully fused thiophene rings could circumvent this problem.⁶ The rigid structure and planarization of the backbone are expected to facilitate molecular ordering through π -stacking, resulting in improved carrier mobilities.^{6,7} Recently, McCulloch et al.⁸ demonstrated organic field effect transistors based on liquid-crystalline regioregular polythiophenes with a pair of fused rings at regular intervals along the polymer backbone, which exhibited charge carrier mobility [$0.6 \text{ cm}^2/(\text{V s})$] close to that of amorphous silicon transistors. The rings “locked the arms” into a flatter shape and made it energetically even easier for neighboring molecules to stack side by side.⁹ According to McCulloch and co-workers,⁸ the fused rings also are harder for oxygen atoms to break apart, making it more resistant to degradation when exposed to air or water, a common problem with conjugated molecules. This gives fused oligothiophenes a competitive edge over other fused conjugated oligomers such as pentacene, which show outstanding charge carrier mobility,¹⁰ but are not environmentally stable, raising concerns over the device lifetime.^{11,12} Thus, fused thiophenes with extended conjugation owing to their planar structures and improved molecular ordering can find potential applications in the field of organic electronics. In fact, Li et al. have reported high charge

carrier mobility and high on/off ratio in thin film transistors based on a material with fused thiophene derivative as building block.¹³ The improved mobility is attributed to π -stacking and macroscopic ordering.¹³

In this paper, we present a systematic spectroscopic study, which compares the electronic structure of nonfused and fused oligothiophene systems incorporated as spacers into platinum containing poly-ynes (Figure 1). The evolution of both the singlet and triplet manifolds with increasing number of fused thiophene units is studied. In order to access the triplet manifold, the oligothiophenes with number of thiophene units, $n = 1, 2$ and 3 are incorporated as bridging ligands (spacers or linker groups) in “rigid-rod” platinum poly-ynes and corresponding monomers, which are commonly used as model compounds to study triplet excited states.^{14–27} The presence of the heavy metal leads to strong spin–orbit coupling and efficient phosphorescence, so that the lowest energy triplet excited-state T_1 becomes spectroscopically accessible.^{15–17} Thus, by combining the platinum poly-yne systems with oligothiophenes (Figure 1), it is possible to probe both the singlet and triplet manifolds of both fused and nonfused oligothiophenes, and draw comparisons between the two classes of materials. The study of triplet excitons is important as they play a significant role in organic photovoltaic cells,^{28,29} in addition to their well-established role in organic light emitting diodes (OLEDs).^{30–32} Triplet excitons in polythiophenes deserve particular attention as they are widely being used in both bulk heterojunction and hybrid solar cells.^{4,5,33} Furthermore, triplet materials (organometallic polymers) have recently been proposed by Wong et al. as a new path toward high-efficiency solar cells.^{34–37} The present study on the effect of chemical modification on singlet and triplet excited states gives an insight into design principles of organic materials for device applications.

By comparing systems with fused and nonfused rings it is possible to assess the effect of planarity on the electronic energy levels of the singlet and triplet excited states. In related studies with polyphenylenes the conjugation length increases when polyphenylenes are linked in a ladder-type structure to give a planar backbone, and consequently, the optical transitions are

* Corresponding authors: E-mails: (A.K.) anna.koehler@uni-bayreuth.de; (M.S.K.) msk@squ.edu.om; (P.R.R.) p.r.raithby@bath.ac.uk.

[†] Cavendish Laboratory, University of Cambridge.

[‡] Department of Physics, University of Bayreuth.

[§] Department of Chemistry, College of Science, Sultan Qaboos University.

^{||} The STFC Daresbury Laboratory.

[⊥] Department of Chemistry, University of Bath.

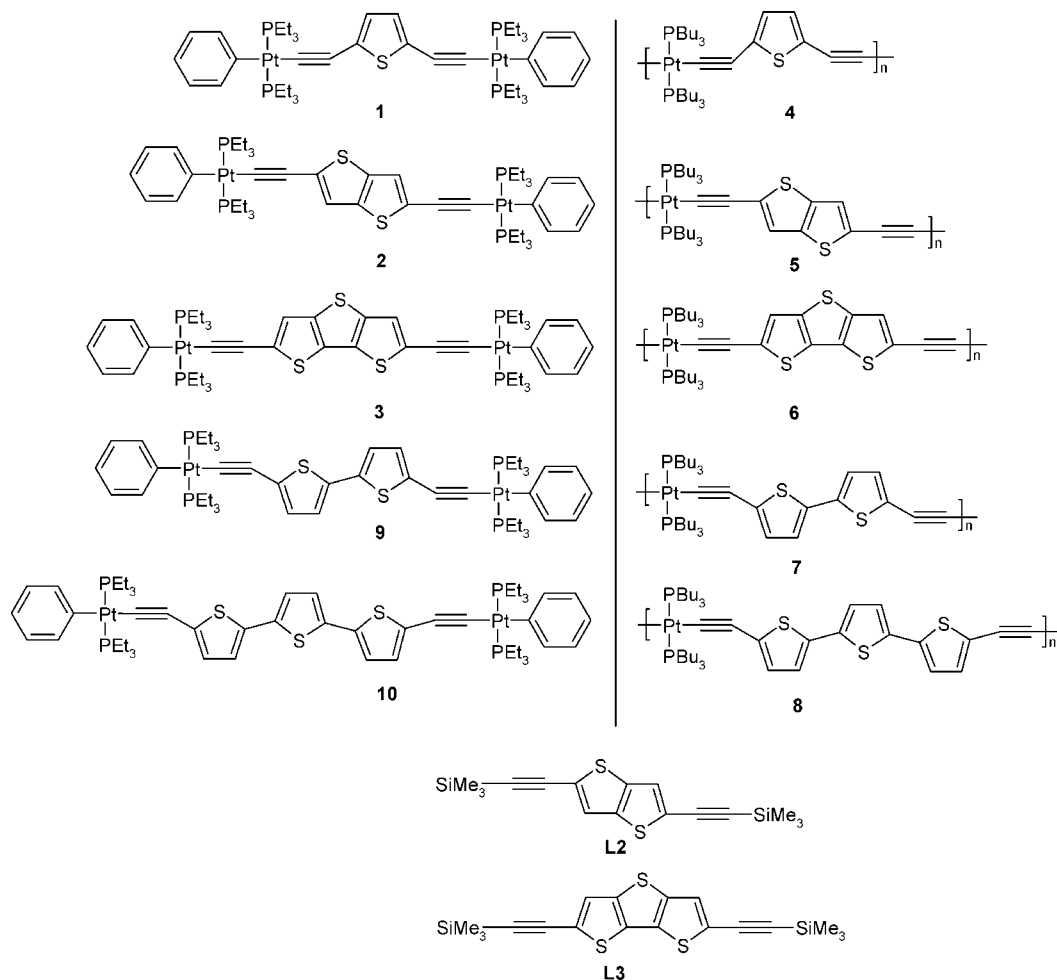


Figure 1. Chemical structures of the monomers (left) and polymers (right) with fused and nonfused oligothiophene spacers. The structures of the fused ligands are also shown.

lowered.^{38,39} For fused thiophene rings, a similar trend could be expected. However, past reports show that the optical gaps in fused polythiophenes are higher than in nonfused polythiophenes with a comparable number of rings.⁴⁰

In order to elucidate the electronic structure of fused oligothiophenes and to compare it against the nonfused counterparts, we investigate a series of platinum containing monomers and polymers containing the linker groups fused thieno[3,2-*b*]thiophene and dithieno[3,2-*b*:2',3'-*d*]thiophene and the nonfused 2,2'-bithiophene and 2,2':5',2''-terthiophene (Figure 1). Monomers with one, two and three fused thiophene rings are named **1**, **2** and **3** respectively and the corresponding polymers are named **4**, **5**, and **6**. The polymers with nonfused thiophene rings are named **7** and **8**. The ligands of the fused thiophene rings are named **L2** and **L3** respectively. The platinum poly-ynes with nonfused bridging ligands have previously been investigated by Chawdhury et al.⁴¹ and some of those previous results are included here for ease of comparison between the two systems.

II. Experimental Section

A. Synthesis. The synthesis of the platinum(II) poly-ynes and diynes with nonfused thiophene rings was reported previously.^{41,42} We here report the synthesis of the systems with the fused thiophene rings. All reactions were performed under a dry argon atmosphere using standard Schlenk or glovebox techniques. Solvents were predried and distilled before use by standard procedures.⁴³ All chemicals and reagents, except where stated otherwise, were obtained from commercial sources and used without further purification. The compounds *trans*-[(Ph)(PEt₃)₂PtCl]⁴⁴ and *trans*-

[(PⁿBu₃)₂PtCl₂]⁴⁵ were prepared by literature procedures. The protected oligothiophenyl dialkynes, 2,5-bis(trimethylsilylethynyl)thieno[3,2-*b*]thiophene and 5,5'-bis(trimethylsilylethynyl)dithieno[3,2-*b*:2',3'-*d*]thiophene were synthesized and purified as described elsewhere.^{46,47} The terminal oligothiophenyl dialkynes, 2,5-bis(ethynyl)thieno[3,2-*b*]thiophene and 5,5'-bis(ethynyl)dithieno[3,2-*b*:2',3'-*d*]thiophene were freshly prepared by proto-desilylation reaction of the protected precursors prior to complexation with the platinum(II) salts.⁴² The NMR spectra were recorded on a Bruker WM-250 or AM-400 spectrometer in CDCl₃. The ¹H and ¹³C{¹H} NMR spectra were referenced to solvent resonances and ³¹P{¹H} NMR spectra were referenced to external trimethylphosphite. IR spectra were recorded as CH₂Cl₂ solutions, in a NaCl cell, on a Perkin-Elmer 1710 FT-IR spectrometer, mass spectra on a Kratos MS 890 spectrometer by the electron impact (EI) and fast atom bombardment (FAB) techniques. Microanalyses were performed in the Department of Chemistry, University of Bath. Preparative TLC was carried out on commercial Merck plates with a 0.25 mm layer of silica. Column chromatography was performed either on silica gel 60 (230 – 400 mesh) or alumina (Brockman grade II–III). Molar masses were determined by GPC method⁴⁸ using two PL Gel 30 cm, 5 μm mixed C columns at 30 °C running in THF at 1 cm³ min⁻¹ with a Roth Mocol 200 high precision pump. A DAWN DSP (Wyatt Technology) multi-angle laser light scattering (MALLS) apparatus with 18 detectors and auxiliary Viscotek model 200 differential refractometer/viscometer detectors was used to calculate the molecular weights (referred to as GPC LS). Thermal analysis (differential thermal analysis, DTA, and thermogravimetry, TG) was performed simultaneously in a Stanton-Redcroft model STA-780 simultaneous thermal analyzer under flowing N₂. Sample masses

were ~1 mg packed with ~1 mg of Al₂O₃ in open Inconel crucibles. The reference crucible contained Al₂O₃. Samples were heated at 10 °C/min to 485 °C. The thermocouple readings were calibrated using a series of DTA standard materials: KNO₃, In, Sn, Ag₂SO₄, and K₂SO₄ as well as Pb and Al as secondary standards, using the same heating rates as the samples.

Preparation of *trans*-[(Ph)(Et₃P)₂Pt-C≡C-R-C≡C-Pt-(PEt₃)₂(Ph)] (*R* = Thieno[3,2-*b*]thiophene-2,5-diyl), **2**. To a stirred solution of *trans*-[(Ph)(PEt₃)₂PtCl] (0.543 g, 1.0 mmol) and 2,5-bisethynylthieno[3,2-*b*]thiophene (0.094 g, 0.5 mmol) in ⁱPr₂NH-CH₂Cl₂ (50 cm³, 1:1 v/v) under nitrogen was added CuI (5 mg). The yellow solution was stirred at room temperature for 15 h., after which all volatile components were removed under reduced pressure. The residue was dissolved in CH₂Cl₂ and passed through a silica column eluting with hexane-CH₂Cl₂ (1:1, v/v). Removal of the solvents *in vacuo* gave the title complex as a pale yellow solid in 70% yield (0.42 g). IR (CH₂Cl₂): ν/cm⁻¹ 2085 (C≡C-). ¹H NMR (250 MHz, CDCl₃): δ 7.53 (s, 2H, =CH), 7.34 (d, 4H, H_{ortho} of Ph), 6.92 (t, 4H, H_{meta} of Ph), 6.77 (t, 2H, H_{para} of Ph), 1.87–1.80 (m, 24H, P-CH₂), 1.10 (m, 36H, P-CH₂CH₃). ¹³C{¹H} NMR (100 MHz, CDCl₃): δ 7.82 (P-CH₂CH₃), 13.18 (P-CH₂), 105.94, 106.76 (C≡C), 119.28, 124.48, 126.93, 127.45, 130.85, 132.54, 135.99, 143.52, 150.08 (aromatic and heteroaromatic). ³¹P{¹H} NMR (101.3 MHz, CDCl₃): δ -131.17, (¹J_{Pt-P} = 2628 Hz). FABMS: *m/z* 1203 (*M*⁺). Anal. Calcd for C₄₆H₇₂P₄S₂Pt₂: C, 45.92; H, 6.03. Found: C, 46.12; H, 5.98.

Preparation of *trans*-[(Ph)(Et₃P)₂Pt-C≡C-R-C≡C-Pt-(PEt₃)₂(Ph)] (*R* = Dithieno[3,2-*b*:2',3'-*d*]thiophene-5,5'-diyl), **3**. This compound was synthesized employing reaction conditions similar to those of **2** but using 5,5'-bis(ethynyl)dithieno[3,2-*b*:2',3'-*d*]thiophene instead of 2,5-bisethynylthieno[3,2-*b*]thiophene. The product was purified on preparative TLC plates with hexane-CH₂Cl₂ (3:7, v/v) as eluent giving the title compound as a yellow solid in an isolated yield of 65%. IR (CH₂Cl₂): ν/cm⁻¹ 2083 (C≡C-). ¹H NMR (250 MHz, CDCl₃): δ 7.38 (s, 2H, =CH), 7.32 (d, 4H, H_{ortho} of Ph), 6.95 (d, 4H, H_{meta} of Ph), 6.80 (t, 2H, H_{para} of Ph), 1.75 (m, 24H, P-CH₂), 1.07 (m, 36H, P-CH₂CH₃). ¹³C NMR (100 MHz, CDCl₃): δ 7.90 (P-CH₂CH₃), 15.22, (P-CH₂), 108.85, 111.01, (C≡C), 119.28, 124.48, 126.93, 127.45, 130.85, 132.54, 135.99, 143.52, 150.08, 156.21 (aromatic and heteroaromatic). ³¹P{¹H} NMR (101.3 MHz, CDCl₃): δ -131.17, (¹J_{Pt-P} = 2653 Hz). FABMS: *m/z* 1259 (*M*⁺). Anal. Calcd for C₄₈H₇₂P₄S₃Pt₂: C, 50.41; H, 6.43. Found: C, 50.69; H, 6.58.

Preparation of *trans*-[(ⁿBu₃P)₂Pt-C≡C-R-C≡C-]_n (*R* = Thieno[3,2-*b*]thiophene-2,5-diyl), **5**. CuI (5 mg) was added to a mixture of *trans*-[Pt(PBu₃)₂Cl₂] (0.670 g, 1.0 mmol) and 2,5-bisethynylthieno[3,2-*b*]thiophene (0.188 g, 1.0 mmol) in ⁱPr₂NH-CH₂Cl₂ (50 cm³, 1:1 v/v). The solution was stirred at room temperature for 15 h, after which all volatile components were removed under reduced pressure. The residue was dissolved in CH₂Cl₂ and passed through a short alumina column. After removal of the solvents by a rotary evaporator, an orange film was obtained readily which was then washed with methanol to give the polymer **5** in 85% isolated yield (0.67 g). Further purification can be accomplished by precipitating the polymer solution in methanol from dichloromethane. IR (CH₂Cl₂): ν/cm⁻¹ 2082 (C≡C-). ¹H NMR (250 MHz, CDCl₃): δ 7.21 (s, 1H, thienothiophene), 6.94 (s, 1H, thienothiophene), 2.17 (m, 12H, P-CH₂), 1.60 (br, 12H, CH₂), 1.41 (sextet, 12H, CH₂), 1.08 (t, 18H, CH₃). ¹³C{¹H} NMR (100 MHz, CDCl₃): δ 13.84 (PCH₂CH₂CH₂CH₃), 23.76–26.35 (PCH₂CH₂CH₂), 111.16, 112.23 (C≡C), 119.48, 132.89, 136.76 (thienothiophene). ³¹P{¹H} NMR (101.3 MHz, CDCl₃): δ -138.03, (¹J_{Pt-P} = 2363 Hz). Anal. Calcd for (C₃₄H₅₆P₂S₂Pt)_n: C, 51.96; H, 7.18. Found: C, 52.09; H, 7.23. GPC (THF): *M*_n = 223 200 gmol⁻¹ (*n* = 284), *M*_w = 401 800 gmol⁻¹, PDI = 1.8.

Preparation of *trans*-[(ⁿBu₃P)₂Pt-C≡C-R-C≡C-]_n (*R* = dithieno[3,2-*b*:2',3'-*d*]thiophene-5,5'-diyl), **6**. This compound was synthesized adopting similar reaction conditions to those of **5** but using 5,5'-bis(ethynyl)dithieno[3,2-*b*:2',3'-*d*]thiophene instead of 2,5-bisethynylthieno[3,2-*b*]thiophene. A brown red solid was obtained in 90% yield. IR (CH₂Cl₂): ν/cm⁻¹ 2081 (C≡C-). ¹H

NMR (250 MHz, CDCl₃): δ 7.26 (s, 1H, dithienothiophene), 6.96 (s, 1H, dithienothiophene), 2.12 (t, 12H, PCH₂), 1.54 (m, 12H, CH₂), 1.48 (br, 12H, CH₂), 1.25 (t, 18H, CH₃). ¹³C{¹H} NMR (100 MHz, CDCl₃): δ 13.84 (PCH₂CH₂CH₂CH₃), 23.76–26.35 (PCH₂CH₂CH₂), 108.39, 110.28 (C≡C), 120.34, 128.52, 129.40, 139.86 (dithienothiophene). ³¹P{¹H} NMR (101.3 MHz, CDCl₃): δ -138.03, (¹J_{Pt-P} = 2373 Hz). Anal. Calcd for (C₃₆H₅₆P₂S₃Pt)_n: C, 51.35; H, 6.70. Found: C, 51.69; H, 6.78. GPC (THF): *M*_n = 222 300 gmol⁻¹ (*n* = 264), *M*_w = 422 400 gmol⁻¹, PDI = 1.9.

B. Crystallography. Data for compounds **2** and **3** were collected using a Bruker AXS SMART CCD area detector on Station 9.8 of the STFC Daresbury Laboratory, equipped with an Oxford Cryostream crystal cooling apparatus. Semiempirical absorption corrections based on interframe scaling were applied. The structures were solved by heavy atom methods and subsequent Fourier difference syntheses and refined by full-matrix least-squares on *F*² (SHELXL 97⁴⁹). Hydrogen atoms were placed in geometrically idealized positions and refined using a riding model. Disorder was observed in both structures. In **2**, there are two molecules in the asymmetric unit, and the terminal phenyl group in one molecule displays positional disorder. The occupancies of these two components were summed to unity. The ethyl phosphine ligands also displayed positional disorder, so where two sites could be distinguished for individual atoms, these were also assigned partial occupancies that were constrained to sum to unity. In the final cycles of refinement a weighting scheme was introduced which produced a relatively flat analysis of variance and refinement was continued until convergence was reached.

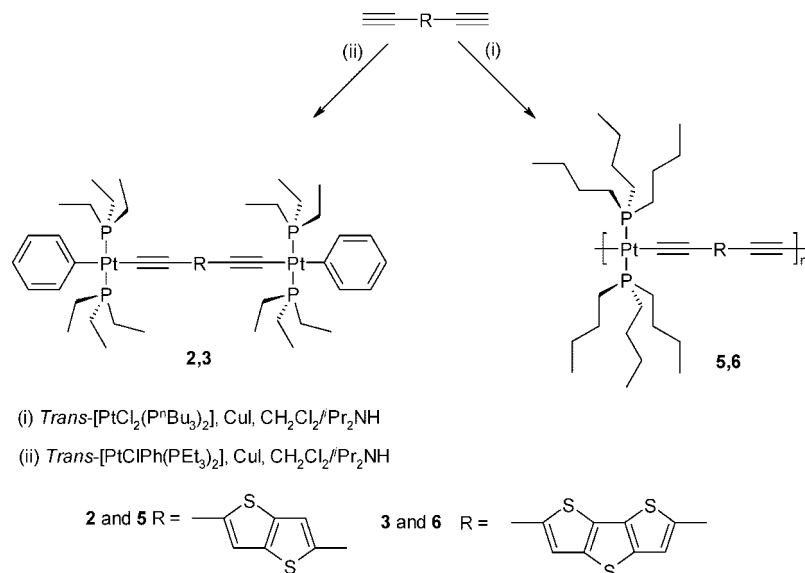
Crystal data: **2** C₄₆H₇₂P₄Pt₂S₂, *M* = 1203.22, triclinic, *P* $\bar{1}$ (No. 2), *a* = 9.0911(6), *b* = 21.0960(13), *c* = 27.6621(7) Å, α = 107.392(1), β = 90.613(1), γ = 101.546(1)°, *V* = 4946.1(5) Å³, *T* = 150(2) K, *Z* = 4, specimen: 0.08 × 0.04 × 0.02 mm, λ = 0.6904 Å, μ = 5.894 mm⁻¹, *T*_{min/max} = 0.489, *N*_{total} = 40214, *N*_{independent} = 25401 [*R*(int) = 0.0327], *wR*₂ = 0.0910 (all data), *R*₁ = 0.0371 (19771 reflections with *I* > 2σ(*I*)); **3** C₄₈H₇₂P₄Pt₂S₃, *M* = 1259.30, Monoclinic, *P*2₁/*c* (No. 14), *a* = 9.3534(12), *b* = 12.4022(16), *c* = 44.475(6) Å, β = 92.129(2)°, *V* = 5155.7(12) Å³, *T* = 150(2) K, *Z* = 4, specimen: 0.16 × 0.10 × 0.01 mm, λ = 0.6904 Å, μ = 5.697 mm⁻¹, *T*_{min/max} = 0.489, *N*_{total} = 40213, *N*_{independent} = 13808 [*R*(int) = 0.0376], *wR*₂ = 0.1660 (all data), *R*₁ = 0.0788 (12453 reflections with *I* > 2σ(*I*))

Crystallographic data (excluding structure factors) have been deposited with the Cambridge Crystallographic Data Centre under the numbers CCDC-xxxxxx-xxxxxx. Copies may be obtained without charge from: CCDC, Union Road, Cambridge CB2 1EZ, U.K. [Fax: internat. +44-1223/336-033; E-mail: deposit@ccdc.cam.ac.uk].

C. Optical Measurements. Films for absorption and luminescence measurements were spin coated from dichloromethane solutions onto quartz substrates by using a conventional photoresist spin-coater. Films were typically 100–150 nm in thickness as measured using a Dektak profilometer. The absorption spectra were taken using Hewlett-Packard ultraviolet–visible (UV–vis) absorption spectrometer.

The photoluminescence (PL) and photoinduced absorption (PIA) spectra were taken with the samples mounted in a continuous flow helium cryostat. The temperature was controlled with an Oxford Intelligent temperature controller-4 (ITC-4). The excitation was provided by the UV lines of a continuous wave (cw) argon ion laser (355–364 nm) with typical intensities of a few mW/mm². The PL spectra were recorded using a spectrograph with an optical fiber input coupled to a cooled charge coupled device (CCD) parallel detection system (Oriel IntraspesIV).

For the PIA spectra, monochromated light from a 150 W tungsten-halogen lamp was used as probe beam. The transmitted probe beam was dispersed through a second monochromator and recorded with a Si-photodiode connected to a SR830 lock-in amplifier. The pump beam provided by the UV lines of a continuous wave (cw) argon ion laser (355–364 nm) was chopped at 125 Hz and the fractional change of transmission in the probe beam was recorded as Δ*T*/*T*. To record the dependence of Δ*T*/*T* on the chopping frequency, this was varied from 4 Hz to 3.5 kHz.

Scheme 1. Synthesis Scheme of Platinum(II) Diynes **2** and **3** and Poly-yne **5** and **6**

III. Results

A. Synthesis and Chemical Characterization. The dehydrohalogenation reactions between *trans*-[(Ph)(Et₃P)₂PtCl] and bis(ethynyl) oligothiophenes (2:1 stoichiometry) in ¹Pr₂NH-CH₂Cl₂, in the presence of CuI at room temperature gave the dinuclear platinum(II) diynes **2** and **3** while the polycondensation reactions between *trans*-[(PⁿBu₃)₂PtCl₂] and the dialkyne (1:1 equivalent) under similar conditions readily afforded the platinum(II) poly-yne **5** and **6** (Scheme 1). The poly-yne were obtained in yields of 85–90%, pointing at a very high conversion. Purification of the platinum(II) diynes was accomplished by column chromatography or preparative TLC on silica while the poly-yne were purified by chromatography on an alumina column.

Initial, systematic characterization of the platinum(II) diynes and poly-yne was achieved by spectroscopic methods. The IR spectra of the platinum(II) diynes and poly-yne show a single sharp $\nu_{C=C}$ absorption at around 2085 cm⁻¹ consistent with a *trans*-configuration of the ethynylene units around the platinum(II) center. ³¹P NMR analyses indicate a well-defined structure for the platinum(II) diynes and poly-yne. In all cases, ¹H resonances arising from the protons of the organic moieties were clearly observed and two distinct ¹³C NMR peaks for the individual ethynylene carbons were observed. The aromatic/heteroaromatic region of the ¹³C NMR spectra reveals a high degree of structural regularity for the main-chain skeleton in the diynes and poly-yne. For example, only 9 well-defined peaks appear in the aromatic and heteroaromatic region, related to the 18 carbon atoms of the symmetric dinuclear platinum(II) diyne compound **2**. Similarly, the ¹³C NMR spectral features of the platinum(II) poly-yne agree with the proposed polymer structures. The resonances due to the ethyl and butyl groups are clearly identified. The single resonance in the ³¹P NMR spectra of the platinum(II) diynes and poly-yne confirms the *trans* arrangement of the phosphine ligands. The ¹J_{Pt-P} values range from 2628 to 2653 Hz for the diynes and 2363–2373 Hz for the poly-yne; the spectral features are similar to other platinum(II) diynes and poly-yne previously reported^{41,42} and confirm the all-*trans* configuration of the compounds.

The mass spectrometric results confirm the molecular assignments for the platinum(II) diynes, **2** and **3**. Gel permeation chromatography (GPC), using a polystyrene (PS) standard shows that the number-average molecular weights of the poly-yne **5** and **6** are in the range of 222 300 to 223 200 g mol⁻¹,

corresponding to degrees of polymerization between 264 and 284. The value of poly dispersity index (PDI) varied between 1.8 and 1.9. The narrow poly dispersity (PDI < 2) in molecular weights is consistent with the proposed linear structure⁵⁰ from the condensation polymerization. GPC data indicate that the number of repeat unit per chain for the thienothiophene-based platinum(II) poly-yne **5** is higher than that for the dithienothiophene-based poly-yne **6** and the degree of polymerization is significantly reduced in both cases as compared to that found for the parent thienylene-based poly-yne **4**. This result reflects significant increase in steric interaction between adjacent repeat units with the number of thienyl rings in Pt(II) poly-yne. The molecular weight values should be viewed with caution in view of the difficulties associated with utilizing GPC for rigid-rod polymers. GPC does not give absolute values of molecular weights but provides a measure of hydrodynamic volume. Rod-like polymers in solution possess very different hydrodynamic properties than flexible polymers. Therefore, calibration of the GPC with PS standards could inflate the values of the molecular weights of the poly-yne to some extent. However, the lack of discernible resonances that could be attributed to end groups in the NMR spectra provides support for the view that high degree of polymerization has been achieved in these organometallic polycondensation reactions.

All samples exhibit an exotherm coincident with mass loss due to decomposition. Decomposition onset was defined as a mass loss of 2%. The peak decomposition temperature was defined as the first inflection point in the thermogravimetric curve, corresponding to a peak in the derivative of the TG data. The decomposition exotherms are broad with multiple peaks, and the TG curves suggest a stepwise process. The first decomposition step corresponds to the removal of trialkylphosphine groups from the Pt(II) diynes and the poly-yne. TG traces show that the Pt(II) diynes and poly-yne have decomposition temperatures of over 380 °C, indicative of excellent thermal stability. These results are quite encouraging as they allow for the use of high temperature sealing procedures in device fabrication. The DTA peaks show exotherms at these temperatures, indicating that decomposition rather than vaporization is being observed. Poly-yne **6** exhibits higher decomposition onset and peak temperatures than **5**, which in turn, exhibits higher thermal stability than the thiophene-containing poly-yne **4**. Similar trend in thermal stability was also observed for the platinum(II) diynes where **3** showed the highest and **1** the lowest

Table 1. Thermal Analysis Results for Decomposition Temperatures of Pt(II) Poly-ynes^a

compound	T_{decomp} (onset)	T_{decomp} (peak)
1	329	365
2	352	379
3	379	422
4	322	355
5	348	372
6	370	414

^a All temperatures in °C. Uncertainties are approximately ± 8 °C.

onset and peak decomposition temperatures. The diynes exhibited slightly higher onset and peak decomposition temperatures than the corresponding platinum(II) poly-ynes. The results are shown in Table 1.

B. Crystallography. In order to establish the exact geometry of the platinum complexes, the crystal and molecular structures of the two complexes, **2** and **3**, were determined. Complex **2** crystallizes in the triclinic space group $P\bar{1}$ with two independent molecules in the asymmetric unit. The two molecules of complex **2** are structurally similar, but one shows disorder of one of the terminal phenyl rings and both show disorder in the ethyl groups. The molecular structure of one of these molecules is illustrated in Figure 2a, but with only one orientation of the disordered unit shown for clarity. The bithiophene group is essentially planar, with an average deviation from the plane of 0.023 Å, and the bond parameters are within the expected range. The two platinum(II) centers within each molecule are square planar, and the PtCPPC square planes make angles of approximately 60° with the central ring system. The bond parameters within the ethynylene metal phosphine fragments are similar to those in other crystallographically characterized diplatinum diyne complexes.^{51–53}

Complex **3** crystallizes in the monoclinic space group $P2_1/c$ with one molecule in the asymmetric unit. The central terthiophene is essentially planar, with a mean deviation from the plane of 0.020 Å, and this group makes dihedral angles of approximately 50° with the planes of the two square planar platinum centers as shown in Figure 2b. The bond parameters within the terthiophene unit do not differ significantly from those in the free ligand,⁴⁷ and the parameters within the two platinum phosphine acetylides units are similar to those in related structures.^{42,51–53}

What is of interest in both structures when considering the electronic properties of these two materials is the absence of $\pi\cdots\pi$ stacking between thiophene rings in adjacent molecules in the crystal which contrasts the situation in related organic materials.¹³ The shortest intermolecular contacts involving the thiophene groups in both structures are between the sulfur atoms and methyl groups on the phosphine ligands of adjacent groups and in the case of **3** an S \cdots S contact of 3.47 Å. The absence of $\pi\cdots\pi$ stacking has also been noted in the structures of the related nonfused bithiophene and terthiophene platinum complexes.⁴² Thus, in both the fused and nonfused platinum complexes the thiophene groups can be considered as being isolated from adjacent thiophenes by the crystal environment and electronic factors that relate to $\pi\cdots\pi$ stacking have been eliminated. Also, while the fused bi- and terthiophene units in **2** and **3** are planar because intramolecular repulsions are already built into the structure the nonfused bithiophene in [PhPt(PET₃)₂-C≡C-(C₄H₂S)-(C₄H₂S)-C≡C-Pt(PET₃)₂Ph] was also found to be planar in the crystalline environment, with a mean deviation from the bithiophene plane of 0.016 Å.⁴² With the *trans* orientation of the two adjacent nonfused thiophene rings there are no short contacts between hydrogen atoms on adjacent ring systems that would prevent planarity, and this conformation is observed in the metal-containing complexes

even when there are no intermolecular $\pi\cdots\pi$ stacking requirements that would favor planarity.

In terms of the conjugation along the molecular backbone, it is of interest to compare the conformations between the platinum centers and the thiophene linker groups. As indicated above the PtP₂C₂ units are square planar and make angles of 60° and 50° with the bi- and terthiophene units in **2** and **3**, respectively. A similar conformation is found in [PhPt(PET₃)₂-C≡C-(C₄H₂S)-(C₄H₂S)-C≡C-Pt(PET₃)₂Ph] where the angles between the PtP₂C₂ square planes and the nonfused bithiophene units for the two independent molecules in the asymmetric unit are 48° and 67°. Thus, in the solid state the crystal packing is probably heavily influenced by the presence of the bulky triethyl- and tributylphosphine ligands, and it would be of interest to compare the conformations with those of the less bulky trimethylphosphine derivatives when these are prepared. In solution, the cylindrical symmetry of, and potential free rotation about the acetylenic units will support conjugation between the thiophene and platinum-containing units that will extend into neighboring repeat units. In consequence, in solution of in a solution-spun amorphous thin film, the lowest-energy conformation is likely to be that with the central thiophene moieties of neighboring repeat units in a planar arrangement, as outlined in ref 20 for similar Pt-Oligomers with a phenyl ring in the bridging ligand, as this gives the highest degree of conjugation along the backbone.

C. Optical Spectroscopy. The thin film absorption spectra of the ligands (**L2** and **L3**), monomers (**2** and **3**) and poly-ynes (**5** and **6**) with two and three fused thiophene rings respectively at room temperature are shown in Figure 3. The absorption spectra of the poly-ynes with nonfused bithiophene and terthiophene spacers (**7** and **8** respectively) are also shown. The energies for the onset of absorption and energy of the 0–0 peak of the singlet emission in solid state for compounds **1** to **8** are summarized in Table 2 to allow comparison between the platinum poly-ynes with fused and nonfused thiophene spacers. The optical gap (i.e., the onset of absorption) decreases with the increasing number of thiophene units in both systems. We attribute this to the increased delocalization of the π -electrons as the number of thiophene units in the bridging ligand (spacer) increases.

The spectral shapes of the ligands **L2** and **L3** are similar to that of monomers **2** and **3** and polymers **5** and **6**, yet the vibronic structure disappears gradually and the onset of absorption shifts to the red from the ligand over the monomer to the polymer. We take this to indicate that the conjugation extends through the platinum atom as observed for the compounds with the nonfused thiophene rings,⁴¹ and that the excited-state has a predominant $\pi-\pi^*$ character.¹⁷ The fact that the energy shifts from ligand to monomer and from monomer to polymer are comparable in the fused thiophene systems and the nonfused systems suggests similar donor–acceptor interaction strength and degree of conjugation in both cases. We note that the absorption band in the compounds based on two or three fused thiophene rings is at higher energy than in the analogous ligands, monomers and polymers with nonfused thiophene spacers.⁴¹

The photoluminescence (PL) spectra of the monomers **2** and **3** and polymers **5** and **6** at 10 K are shown in Figure 4a. The PL spectra of polymers **7** and **8** (with nonfused spacers with two and three thiophene units respectively) are also plotted from ref 33 for the ease of comparison. All spectra show two emission bands. The emission bands at higher energies (above 2.0 eV) are attributed to the same singlet state that gives rise to the main absorption band in Figure 3. The lower energy emission peaks, indicated in the figure by arrows, are assigned to a triplet excited state (phosphorescence); its well-resolved vibronic structure in polymers **5** and **6** is similar to the singlet emission and excludes an excimer origin.

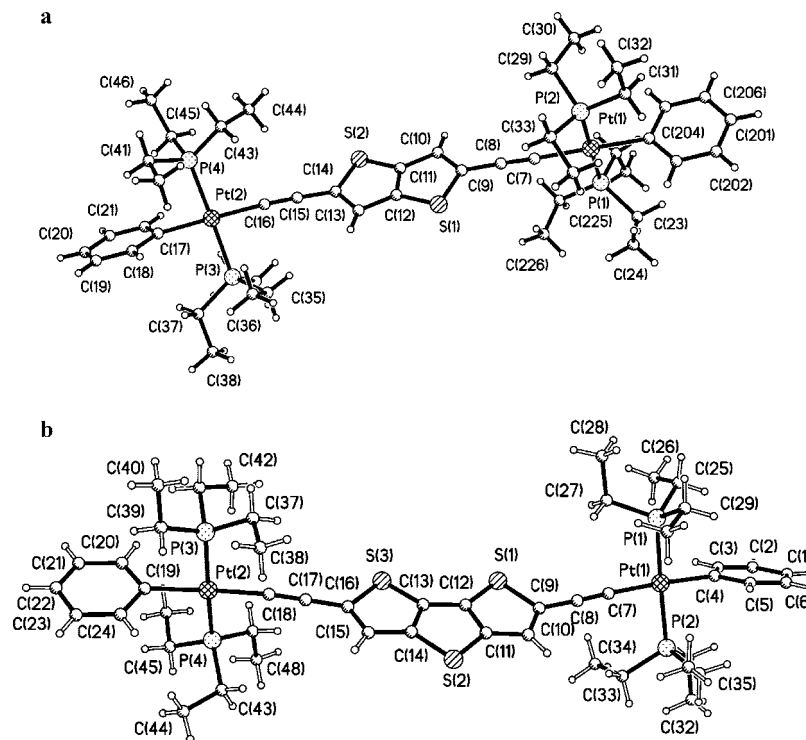


Figure 2. Molecular structures of (a) complex **2** and (b) complex **3**. Both diagrams show the atom numbering scheme used but only one orientation of the disordered component in **2** is shown for clarity. Also for **2** only one of the two independent but structurally similar molecules is shown.

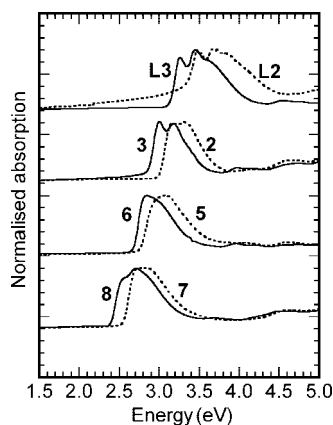


Figure 3. Optical absorption spectra taken from thin films of the ligands (referred to as **L2** and **L3**), monomers **2** and **3** and the polymers **5** and **6** with fused thiophene spacers at room temperature are shown. For the ease of comparison, the spectra of polymers **7** and **8** with nonfused spacers are also plotted from ref 41. The dotted lines denote the systems with two thiophene rings and solid lines denote the systems with three thiophene rings as spacer.

Table 2. Energies of the Onset of Absorption and the 0–0 Vibrational Peak of Emission for the Pt(II) Poly-yne with Fused Thiophenes

compound	onset of absorption (eV)	energy of the 0–0 peak in the emission spectra (eV)
1 ⁶⁸	3.14	3.10
2	3.02	2.99
3	2.89	2.86
4 ⁴¹	2.86	2.85
5	2.78	2.76
6	2.68	2.67

There is little energy difference between the 0–0 peak of the phosphorescence between the monomer and corresponding polymer, i.e. between **2** and **5** or between **3** and **6**. As observed

for related compounds, this suggests the triplet excited-state to be confined to one repeat unit, i.e. the two or three thiophene rings between the ethynylene units. From Figure 4, both singlet and triplet emission red shift in parallel in monomeric and polymeric systems as the number of thiophene rings within the bridging ligand increases such that a constant singlet–triplet energy gap (exchange energy) is maintained. The triplet emission is shifted by about 0.8 eV from the singlet excited-state as observed for the analogous polymers **7** and **8**⁴¹ with nonfused spacers and a large number of other Pt-containing polymers.¹⁶ Another important observation from Figure 4 is that the polymers based on fused thiophene spacers are blue-shifted compared to the nonfused counterparts. The origin of this will be discussed later.

Figure 4b shows the room temperature emission spectra of the monomers **2** and **3** and polymers **5** and **6**. The spectra are inhomogeneously broadened so that the vibrational structure is reduced. For the polymers, the phosphorescence can no longer be observed. We attribute this to diffusion of the triplet exciton to dissociation states along the polymer chain.¹⁴ It is interesting to note that the 0–0 peaks of the phosphorescence at 10 K and at 300 K coincides for the fused monomer **2**. In Pt–acetylide compounds, in particular for short oligomers, the conjugated moieties on the bridging ligands that form neighboring repeat units may arrange in a planar or a perpendicular fashion. In the planar arrangement, conjugation is largest and so this is the lowest energy state. Under certain preparation conditions, emission from the higher-energy perpendicular conformation can be observed at low temperatures yet disappears at temperatures above 100 K due to energy transfer to a lower energy planar conformation.²⁰ The coincidence of the 10 K and 300 K phosphorescence maxima here suggests the emission to originate from the lowest energy conformation, probably with the phenyl end groups and the fused thiophene moiety in one plane such as to maximize conjugation. We note that this may be different from the conformation one obtains in a crystal structure, where the interaction with neighboring molecules plays a larger contribution. For compounds **1** and **4**, temperature dependent

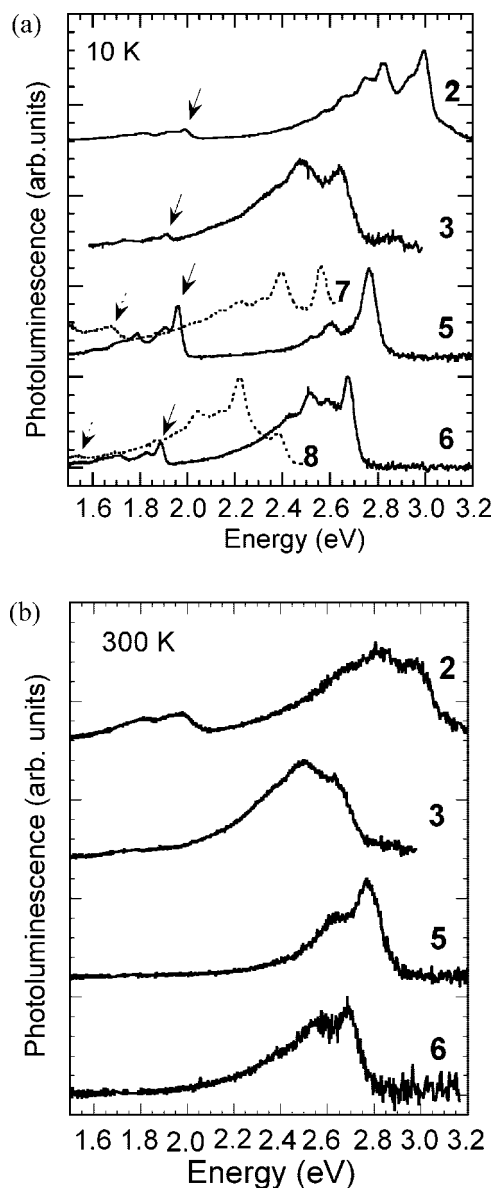


Figure 4. Photoluminescence spectra taken from thin films of monomers **2** and **3** and the polymers **5** and **6** (a) at 10 K and (b) at 300 K. The 10 K spectra of polymers **7** and **8** are also plotted (dotted lines) from ref 41 for comparison. In the 300 K spectra, some stray laser light from the 2nd order transmission of the grating around 1.7 eV has been cut out from the spectra.

phosphorescence measurement did not show any sign of a higher energy conformation.^{41,58} For the polymers **5**, **6**, **7**, and **8**, the intensity of the phosphorescence signal is too low to allow for a detailed temperature-dependent study. The shape of the 10 K spectra does not show any discernible high energy shoulder. We therefore consider that in the compounds studied here, phosphorescence is most likely from the lowest energy conformation.

The intensity of the triplet emission decreases with increasing number of thiophene rings, i.e., there are either less triplets generated when going from the bithiophene to the terthiophene ligand, or more of them decay nonradiatively. In purely organic oligothiophenes, the triplet generation by intersystem crossing reduces from bithiophene to terthiophene.^{54,55} This is because in a purely organic bithiophene, the energy of the S_1 singlet is just slightly above the energy of a T_4 triplet state. This result in an intersystem crossing rate due to vibrational spin-orbit coupling that is relatively large for an organic compound. In contrast, for terthiophene, the S_1 energy level falls below that

of the T_4 triplet energy so intersystem crossing is reduced.^{54,55} In our organometallic compounds, the intersystem crossing is dominated by heavy-atom induced spin orbit coupling, and so the ideal energy match for vibrational spin-orbit coupling is unlikely to play a significant role. The other factor that can reduce the triplet state population, the nonradiative decay via internal conversion, follows the “energy gap law” which states that the nonradiative decay rate increases with decreasing energy of the triplet state.¹⁵ When considering the 0–0 energies of the phosphorescence in polymers **5** and **6** shown in Figure 4, the relative intensities agree well with the trend that was established for a number of closely related Pt-polymers and that is based on the energy gap law.¹⁵ Furthermore, the phosphorescence intensity is weaker for the monomers than for the polymers, as observed earlier for related complexes.¹⁵

We now draw attention to the vibronic structure in the *singlet* emission band of the polymers **5** and **6** and monomers **2** and **3** (see Figure 4). The vibronic structure changes significantly when going from the two fused ring system to the three fused ring system. For two fused rings, the 0–0 peak is dominant, while for three fused rings, the higher vibronic peaks gain weight. This suggests a much more profound geometric distortion to occur upon excitation for three fused thiophene rings than for two. (According to Beljonne et al.,⁵⁶ the ethylenic units are rigid with respect to photoexcitations, so that most of the relaxations must occur on the aromatic ring between the ethynylene units). There is also more weight in the vibronic side-peaks in the monomers **2** and **3** than in the polymers **5** and **6**. The stronger geometric distortion of the excited-state in the monomer than in the polymer suggests the singlet excited-state extends over several repeat units in the polymer. This is in agreement with the bathochromic shift of the absorption and emission from monomer to polymer. It should be noted that in **3**, the peak at 2.86 eV is assigned to the 0–0 peak, as this is consistent with the small energy gap between the 0–0 peak of emission and the onset of absorption observed for **5**, **6**, and **2** (see Table 2). We note that in **3**, the intensity of the 0–0 peak is extremely low compared to other compounds.

The vibronic structure of polymers with nonfused⁴¹ and fused thiophene spacers are compared in parts a and b of Figure 5, respectively by aligning the 0–0 peak of emission on the energy axis. From Figure 4, we can see that for compound **7**, the 0–0 peak and the vibronic side peak have almost the same intensity while for compound **8**, the intensity of the 0–0 peak is less and the vibronic peak gains weight. On the other hand, for the fused polymers **5** and **6**, the intensity of the vibronic side peaks are always less compared to the 0–0 peak (Figure 5b). This indicates that they are less distorted compared to the nonfused ones due to their more rigid structure.

The photoinduced absorption spectra of the monomers with two and three fused thiophene units (**2** and **3**) are shown in Figure 6a. At 10 K, we observe only one peak for monomer **2** (at energy 2.16 eV) while there are two peaks for **3** (at energies 1.6 and 2.05 eV). The low energy peak at 1.6 eV disappears at room temperature, whereas the high-energy peak at 2.05 eV is reduced to approximately a third of the intensity at 10 K. In order to unambiguously assign the $T_1 \rightarrow T_n$ transition, we measured the dependence of the signal intensity on the chopping frequency of the pump beam and the data is displayed in Figure 6c. A theoretical fit corresponding to monomolecular decay equation, $S(\omega, \tau) = A\tau/(1 + \omega^2\tau^2)^{1/2}$ (where $S(\omega, \tau)$ is the magnitude of the PIA signal, A is a constant and τ is the lifetime of a single species)⁵⁷ is also shown in Figure 6c. A good fit can be obtained for the peak at 2.05 eV with a lifetime of $55 \pm 5 \mu\text{s}$ for **3** at 10 K. According to the energy-gap law, the lifetime of phosphorescence depends strongly on the internal conversion rate¹⁵ and thus on the energy of the triplet state. In other words,

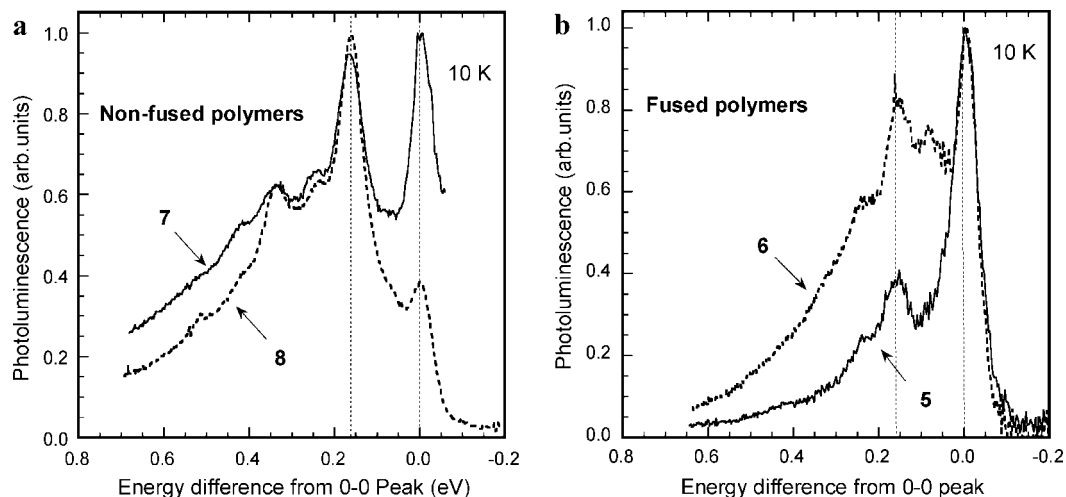


Figure 5. Singlet emission with the intensity of 0–0 peak normalized to unity on the ordinate and the energy of the 0–0 peak set to 0 eV on the abscissa at 10 K (a) for polymers **7** and **8** with nonfused spacers with two and three thiophene units respectively (taken from ref 33) and (b) for polymers **5** and **6** with fused thiophene spacers.

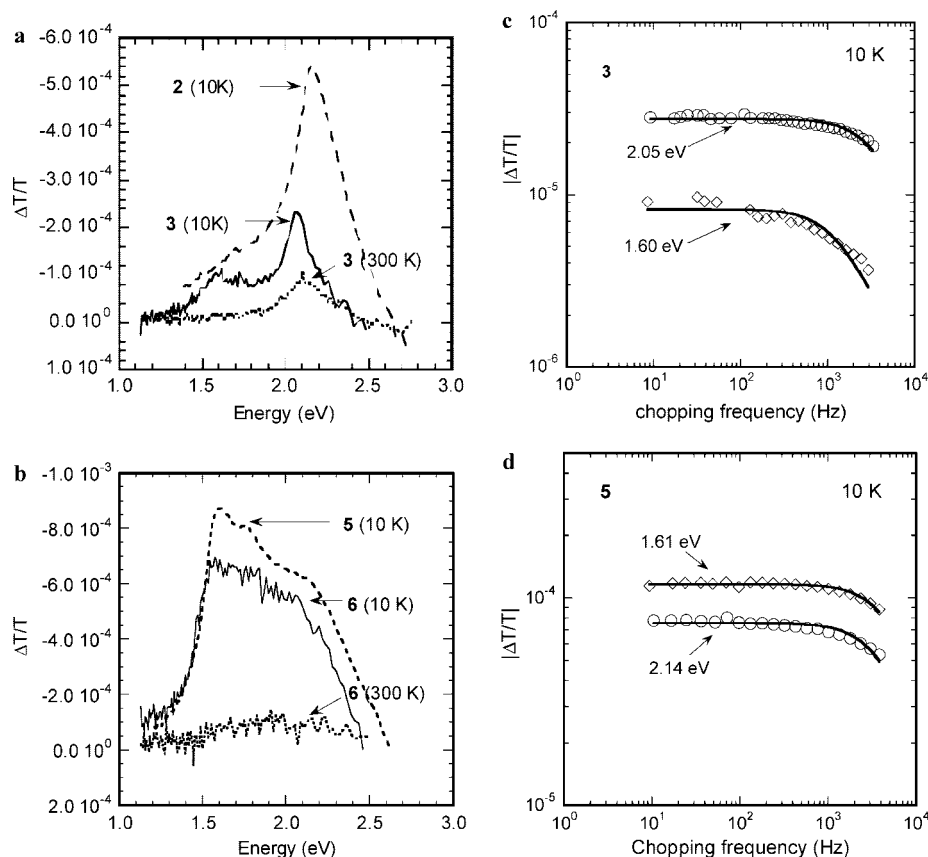


Figure 6. Steady state photoinduced absorption spectra from thin solid films (a) for the monomers **2** (at 10 K) and **3** (at 10 and 300 K) and (b) for the polymers **5** (at 10 K) and **6** (at 10 and 300 K) as indicated in the figure (The spectrum of **5** was divided by 5 for ease of comparison). (c) and (d) The frequency dependence of the photoinduced absorption for monomer **3** at 2.05 eV (circles) and at 1.60 eV (diamonds) and polymer **5** at 2.14 eV (circles) and at 1.61 eV (diamonds) measured at 10 K, respectively. The solid lines indicate the fits as described in the text.

as the energy of the triplet excited-state decreases the phosphorescence lifetime also decreases. A lifetime of 55 μs for the triplet state at 2.05 eV in **3** is consistent with the lifetime of 41 μs found in a related platinum poly-yne polymer with a $T_1 - T_0$ energy of 1.85 eV.¹⁵ In contrast, the peak at 1.6 eV corresponds to a lifetime of $140 \pm 10 \mu\text{s}$, which is too long considering the low energy of the triplet state. Furthermore, the $T_1 \rightarrow T_n$ transition in a related platinum monomer with one phenyl, thiophene or pyridine spacers was found between 2.0 and 2.2 eV.⁵⁸ We therefore attribute the 2.05 eV peak to the

$T_1 \rightarrow T_n$ transition. Similarly, the monomolecular decay equation gives a lifetime of $53 \pm 5 \mu\text{s}$ for the peak at 2.16 eV for monomer **2** (not shown). The origin of the peak at 1.6 eV in **3** is unclear. We speculate that it might be of some polaronic origin.

Figure 6b shows the photoinduced absorption spectra of polymer **5** at 10 K and **6** at 10 K and at room temperature. Both compounds show a peak around 1.6 eV with a very broad shoulder extending to 2.0 eV. This shoulder remains at room temperature, while the feature around 1.6 eV disappears. For

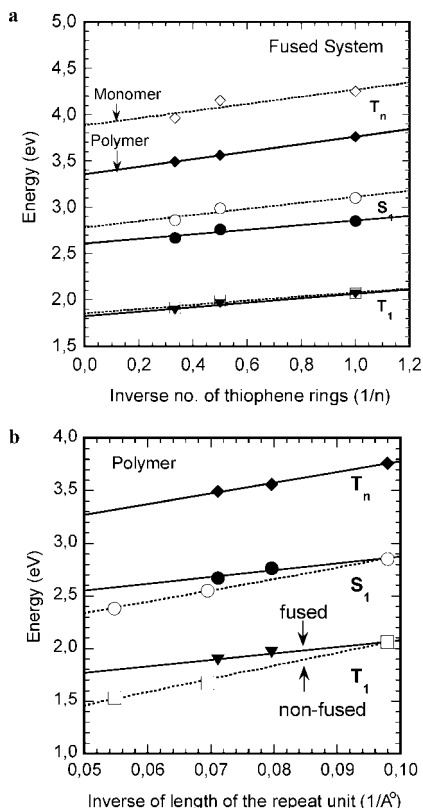


Figure 7. (a) Singlet (S₁) and triplet (T₁, T_n) excited-state energies in the monomers (dotted lines) and polymers (solid lines) with fused thiophene spacers plotted against the inverse number of thiophene units within the bridging ligand. (b) Singlet and triplet energies against the inverse length of repeat unit for the polymers with fused (solid line) and nonfused (dashed line) thiophene spacers. (The energy levels in nonfused systems are taken from ref 41).

an analogous platinum poly-yne polymer with a single thiophene unit as spacer (compound **4** in Figure 1),⁵⁸ a similar temperature dependence has been observed for PIA signal peak at 1.7 eV. In a related Pt-polymer with a phenyl spacer, a photoinduced absorption feature at 1.5 eV was attributed to the T₁ → T_n transition on the basis of lifetime measurements.^{56,59} We therefore consider the feature at 1.6 eV to be the T₁ → T_n transition, while the broad shoulder may be of a different origin such as a polaron. Moreover, for **5**, the monomolecular fit of the frequency dependence of PIA signal intensity gives a lifetime of 39 ± 5 μs for the peak at 1.61 eV while it gives a value of 48 ± 6 μs for the shoulder at 2.14 eV (Figure 6d). For a triplet state in platinum containing poly-yne at this particular triplet energy (1.6 eV), a lifetime of 33 ± 5 μs is previously reported,¹⁵ so the peak around 1.6 eV is more likely to be the T₁ → T_n absorption in polymers **5** and **6**. It should be noted that the intensity of the photoinduced absorption is stronger for the polymers and monomers with two thiophene rings than with three thiophene rings. This is due to the higher energy and therefore increased lifetime of the T₁ triplet state from which the absorption occurs.¹⁵

IV. Discussion

The photoluminescence and photoinduced absorption measurements allow us to determine the energy levels of singlet (S₁) and triplet (T₁ and T_n) excited states in monomers **2** and **3** and polymers **5** and **6** with fused thiophene rings. A comparison between the energy levels in the monomers and polymers in the fused systems is plotted in Figure 7a as inverse function of the number of thiophene units within the bridging ligand. The energy levels of polymer with a single thiophene spacer

(compound **4**) is also included in Figure 7a for comparison. It can be seen that the lowest triplet excited state, T₁, is localized on one repeat unit, while the S₁ and T_n states extend over a few repeat units. As mentioned before, the singlet-triplet exchange energy (S₁-T₁) remains constant in polymers **5** and **6** irrespective of the number of thiophene units within the spacer.

A constant exchange energy in platinum poly-ynes with oligothiophene spacers is in contrast to the reduction of singlet-triplet energy gap (S₁-T₁) in purely organic oligothiophenes with increasing number of thiophene units as reported by Beljonne et al.^{54,55,60,61} The difference is due to a "spatial confinement effect" that occurs for oligothiophenes, yet not for the platinum polymers. In conjugated polymers, a singlet (triplet) excited-state consists of one electron in the π and another one with opposite (same) spin in the π* frontier orbitals. In the triplet state, the motion of the two electrons are better correlated and so the overall extent of the triplet exciton is smaller than that of the singlet exciton.⁶² A decreasing oligomer length thus confines the singlet more strongly than the triplet and so the singlet energy rises more strongly than the triplet energy with decreasing oligomer size. Consequently, the exchange energy increases. This is well-known and also applies for oligothiophenes.^{54,55,60,61} In contrast, in the platinum polymers considered here, the thiophene oligomers are embedded between two ethynylene units followed by a platinum atom. While the bond between the heavy metal and the organic ligand may not be as conjugated as a carbon-carbon bond, it still allows for some degree of conjugation between neighboring units, as is evident from the red shift in S₁ and T_n energies from monomer to polymer (Figure 7a). Changing the number of thiophene rings alters the electron density of the ligand and therefore the overall transition energy, yet it does not spatially confine the excited singlet or triplet state wave functions. In consequence, singlet and triplet evolve in parallel.

In order to make a comparison between the *fused* and *nonfused* thiophene systems, the energy levels of singlet (S₁) and triplet (T₁ and T_n) excited states are plotted against the inverse length of repeat unit (obtained from X-ray diffraction measurements) in Figure 7b. We observe that the energies of the first singlet (S₁) and triplet (T₁) excited states are higher in the fused systems than in the nonfused systems. This is in contrast to the evolution observed for poly(*p*-phenylene) type systems. Poly(*p*-phenylene)s are characterized by some torsion between adjacent phenyl rings due to steric hindrance between the hydrogen atoms on adjacent phenyl rings. Connecting phenylene rings as in the ladder-type MeLPPP enforces planarity on the poly(*p*-phenylene) backbone and the associated the π-conjugated system and so reduces the S₀ → S₁ and S₀ → T₁ transition energies.³⁸ Between adjacent thiophene units, such a steric hindrance does not occur. In fact, in a crystalline environment, the thiophene rings may even adopt a planar conformation. This was observed by X-ray measurements for the nonfused Pt-monomers **9** and **10** and for polythiophene and oligothiophene crystallites.^{1,42,63,64} Nevertheless, in amorphous thin films this energetically favorable state is not reached, and polythiophenes are well-known to adopt a coiled conformation with torsions between adjacent rings.^{1,65-67} In a similar way, in the amorphous films that result from spin-coating out of a dichloromethane solution with a boiling point around 40 °C, there is likely to be some torsion between the rings in the nonfused platinum systems. On the basis of a planarity argument of the π-conjugated system, the excited states in Pt compounds with the fused thiophenes should therefore be at lower energy, contrary to what is observed.

In order to understand why excited states in the fused systems are at higher energy than in the nonfused analogues, it is instructive to take a close look at the chemical structure of the

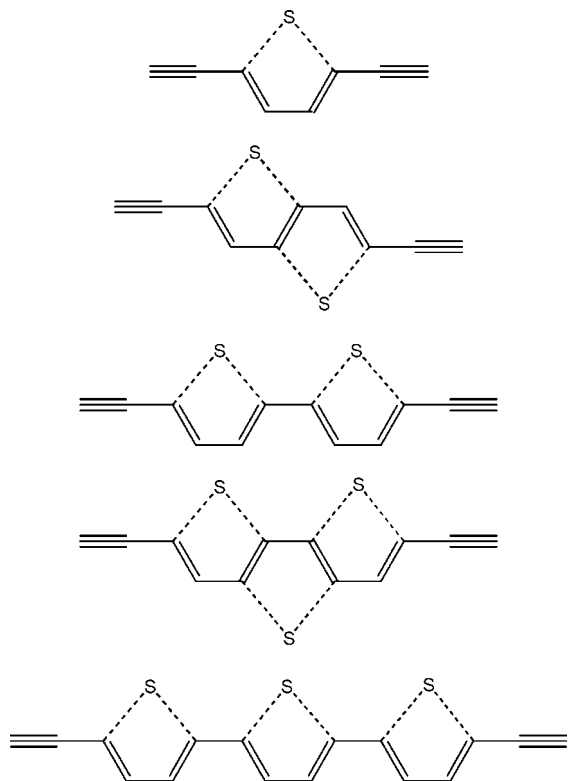


Figure 8. Schematic showing the number of double bonds within the fused and nonfused oligothiophene spacers.

conjugated ligand, as illustrated in Figure 8. The energy shift in the absorption band from the monomers to the polymers (see Table 2) clearly demonstrates that conjugation extends through the platinum group, yet the main contribution to the delocalization in the π -conjugated system arises from the oligothiophene spacer. Most of the conjugation occurs via the alternating carbon–carbon bonds, with little involvement from the sulfur atom. When two thiophene rings are fused, this reduces the number of double bonds from four to three (or from six to four when fusing three rings) and therefore reduces the conjugation of the system significantly. We consider this to be the main cause for the increase in the excited-state transition energies. We note that the higher energy in the fused systems is not just caused by a shorter spacer length as is evident from Figure 7b. To exclude possible confinement effects, we displayed the excited-state energies as a function of inverse spacer length and fitted them to straight lines with good agreement. For a given spacer length, the measured and any extrapolated transition energies for the fused systems are always at higher energies. In addition to the number of double bonds, the sulfur atom seems to contribute a secondary effect. When comparing polymers **6** (with three fused rings) and **7** (with two nonfused rings), which have the same number of double bonds, we still find a higher energy of the optical transitions in the fused polymer than in the nonfused polymer (see Figure 7b). The difference could be caused by the presence of the additional sulfur atom that affords additional electron density to the bonding molecular orbitals (HOMO). We therefore speculate, a lowered HOMO level may result in an increased energy of the optical transitions in fused systems. However, quantum chemical calculations would be required to resolve this.

V. Summary

We compared the properties of singlet (S_1) and triplet (T_1) excited states in fused and nonfused oligothiophenes by incorporating them into platinum poly-ynes. We find that the

energies of the optical transitions for the singlet and triplet excited states shift to higher energies when going from the nonfused to the fused systems, despite the planarity of the fused system. The shift in electronic energies to higher values in fused system compared to nonfused system with same number of thiophene rings is attributed to the level of conjugation within the oligothiophene spacers. The greater the number of conjugated double bonds, the lower is the energy gap. Secondary effects can be attributed to the presence of the additional sulfur atoms in the fused thiophene systems compared to their nonfused counterparts, which further widens the HOMO–LUMO energy gap.

Acknowledgment. We acknowledge funding from the Cambridge Commonwealth Trust (L.S.D.), Royal Society (A.K.), Sultan Qaboos University, Sultanate of Oman (M.S.K.), EPSRC for a Senior Research Fellowship (P.R.R.) and a studentship (H.A.S.) and the Cambridge Crystallographic Data Centre (L.M.).

References and Notes

- (1) Fichou, D. *Handbook of Oligo- and Polythiophene*; Wiley-VCH: Weinheim, Germany, and New York, 1999.
- (2) Dodabalapur, A.; Torsi, L.; Katz, H. E. *Science* **1995**, *268*, 270.
- (3) Horowitz, G.; Deloffre, F.; Garnier, F.; Hajlaoui, R.; Hmyene, M.; Yassar, A. *Synth. Met.* **1993**, *54*, 435.
- (4) Kim, Y.; Cook, S.; Tuladhar, S. M.; Choulis, S. A.; Nelson, J.; Durrant, J. R.; Bradley, D. D. C.; Giles, M.; Mc Culloch, I.; Ha, C.-S.; Ree, M. *Nat. Mater.* **2006**, *5*, 197.
- (5) Li, G.; Shrotriya, V.; Huang, J.; Yao, Y.; Moriarty, T.; Emery, K.; Yang, Y. *Nat. Mater.* **2005**, *4*, 864.
- (6) Zhang, X.; Cote, A. P.; Matzger, A. J. *J. Am. Chem. Soc.* **2005**, *127*, 10502.
- (7) Holmes, D.; Kumaraswamy, S.; Matzger, A. J.; Vollhardt, K. P. C. *Chem. Eur. J.* **1999**, *5*, 3399.
- (8) McCulloch, I.; Heeney, M.; Bailey, C.; Genevicius, K.; MacDonald, I.; Shkunov, M.; Sparrowe, D.; Tierney, S.; Wagner, R.; Zhang, W.; Chabinyac, M. L.; Kline, J.; McGehee, M. D.; Toney, M. F. *Nat. Mater.* **2006**, *5*, 328.
- (9) Service, R. F. *Science* **2006**, *311*, 1691.
- (10) Dimitrakopoulos, C. D.; Malenfant, P. R. L. *Adv. Mater.* **2002**, *14*, 99.
- (11) Yamada, M.; Ikemoto, I.; Kuroda, H. *Bull. Chem. Soc. Jpn.* **1988**, *61*, 1057.
- (12) Bredas, J. L.; Calbert, J. P.; Filho, D. A. d. S.; Cornil, J. *PNAS* **2002**, *99*, 5804.
- (13) Li, X.-C.; Sirringhaus, H.; Garnier, F.; Holmes, A. B.; Moratti, S. C.; Feeder, N.; Clegg, W.; Teat, S. J.; Friend, R. H. *J. Am. Chem. Soc.* **1998**, *120*, 2206.
- (14) Sudha Devi, L.; Al-Suti, M. K.; Dosche, C.; Khan, M. S.; Friend, R. H.; Köhler, A. *Phys. Rev. B* **2008**, *78*, 045210.
- (15) Wilson, J. S.; Chawdhury, N.; Al-Mandhary, M. R. A.; Younus, M.; Khan, M. S.; Raithby, P. R.; Köhler, A.; Friend, R. H. *J. Am. Chem. Soc.* **2001**, *123*, 9412–9417.
- (16) Köhler, A.; Wilson, J. S.; Friend, R. H.; Al-Suti, M. K.; Khan, M. S.; Gerhard, A.; Bässler, H. *J. Chem. Phys.* **2002**, *116*, 9457–9463.
- (17) Köhler, A.; Beljonne, D. *Adv. Funct. Mater.* **2004**, *14*, 11.
- (18) Silverman, E. E.; Cardolaccia, T.; Zhao, X. M.; Kim, K. Y.; Haskins-Glusac, K.; Schanze, K. S. *Coord. Chem. Rev.* **2005**, *249*, 1491–1500.
- (19) Schanze, K. S.; Silverman, E. E.; Zhao, X. M. *J. Phys. Chem. B* **2005**, *109*, 18451–18459.
- (20) Glusac, K.; Kose, M. E.; Jiang, H.; Schanze, K. S. *J. Phys. Chem. B* **2007**, *111*, 929–940.
- (21) Cardolaccia, T.; Li, Y. J.; Schanze, K. S. *J. Am. Chem. Soc.* **2008**, *130*, 2535–2545.
- (22) Wong, W. Y.; Choi, K. H.; Lu, G. L.; Shi, J. X. *Macromol. Rapid Commun.* **2001**, *22*, 461–465.
- (23) Cooper, T. M.; Blaudau, J. P.; Hall, B. C.; Rogers, J. E.; McLean, D. G.; Liu, Y. L.; Toscano, J. P. *Chem. Phys. Lett.* **2004**, *400*, 239–244.
- (24) Cooper, T. M.; Krein, D. M.; Burke, A. R.; McLean, D. G.; Rogers, J. E.; Slagle, J. E. *J. Phys. Chem. A* **2006**, *110*, 13370–13378.
- (25) Cooper, T. M.; Krein, D. M.; Burke, A. R.; McLean, D. G.; Rogers, J. E.; Slagle, J. E.; Fleitz, P. A. *J. Phys. Chem. A* **2006**, *110*, 4369–4375.
- (26) Rogers, J. E.; Hall, B. C.; Hufnagle, D. C.; Slagle, J. E.; Ault, A. P.; McLean, D. G.; Fleitz, P. A.; Cooper, T. M. *J. Chem. Phys.* **2005**, *122*.
- (27) Slagle, J. E.; Cooper, T. M.; Krein, D. M.; Rogers, J. E.; McLean,

- D. G.; Urbas, A. M. *Chem. Phys. Lett.* **2007**, *447*, 65–68.
- (28) Köhler, A.; Wittmann, H. F.; Friend, R. H.; Khan, M. S.; Lewis, J. *Synth. Met.* **1996**, *77*, 147–150.
- (29) Yang, C.-M.; Wu, C.-H.; Liao, H.-H.; Lai, K.-Y.; Cheng, H.-P.; Hornga, S.-F. *Appl. Phys. Lett.* **2007**, *90*, 133509.
- (30) Baldo, M. A.; O'Brien, D. F.; You, Y.; Shoustikov, A.; Sibley, S.; Thompson, M. E.; Forrest, S. R. *Nature* **1998**, *395*, 151.
- (31) Adachi, C.; Baldo, M. A.; Forrest, S. R.; Lamansky, S.; Thompson, M. E.; Kwong, R. C. *Appl. Phys. Lett.* **2001**, *78*, 1622.
- (32) Cleave, V.; Yahioglu, G.; Le Barny, P.; Friend, R. H.; Tessler, N. *Adv. Mater.* **1999**, *11*, 285.
- (33) Beek, W. J. E.; Wienk, M. M.; Janssen, R. A. J. *Adv. Funct. Mater.* **2006**, *16*, 1112.
- (34) Wong, W. Y.; Wang, X. Z.; He, Z.; Djuricic, A. B.; Yip, C. T.; Cheung, K. Y.; Wang, H.; Mak, C. S. K.; Chan, W. K. *Nat. Mater.* **2007**, *6*, 521–527.
- (35) Shao, Y.; Yang, Y. *Adv. Mater.* **2005**, *17*, 2841.
- (36) Guo, F. Q.; Kim, Y. G.; Reynolds, J. R.; Schanze, K. S. *Chem. Commun.* **2006**, 1887, 1889.
- (37) Wong, W. Y.; Wang, X. Z.; He, Z.; Chan, K. K.; Djuricic, A. B.; Cheung, K. Y.; Yip, C. T.; Ng, A. M. C.; Xi, Y. Y.; Mak, C. S. K.; Chan, W. K. *J. Am. Chem. Soc.* **2007**, *129*, 14372–14380.
- (38) Hertel, D.; Setayesh, S.; Nothofer, H.-G.; Scherf, U.; Müllen, K.; Bässler, H. *Adv. Mater.* **2001**, *13*, 65–70.
- (39) Oyaizu, K.; Iwasaki, T.; Tsukahara, Y.; Tsuchida, E. *Macromolecules* **2004**, *37*, 1257.
- (40) Roncali, J. *Chem. Rev.* **1997**, *97*, 173.
- (41) Chawdhury, N.; Köhler, A.; Friend, R. H.; Wong, W.-Y.; Younus, M.; Raithby, P. R.; Lewis, J.; Al-Mandhury, M. R. A.; Coreoran, Y. C.; Khan, M. S. *J. Chem. Phys.* **1999**, *110*, 4963–4970.
- (42) Lewis, J.; Long, N. J.; Raithby, P. R.; Shields, G. P.; Wong, W. Y.; Younus, M. *J. Chem. Soc., Dalton Trans.* **1997**, 4283, 4288.
- (43) Armarego, W. L. F.; Perrin, D. D. Purification of laboratory chemicals, 4th ed.; Butterworth-Heinemann: Guildford, U.K., 1996.
- (44) Siegmann, K.; Pregosin, P. S.; Venanzi, L. M. *Organometallics* **1989**, *8*, 2659–2664.
- (45) Kaufman, G. B.; Teter, L. A. *Inorg. Synth.* **1963**, *7*, 248–252.
- (46) Khan, M. S.; Al-Naamani, R. S.; Ahrens, B.; Raithby, P. R. *Acta Crystallogr.* **2004**, *E60*, 01202–01203.
- (47) Khan, M. S.; Ahrens, B.; Raithby, P. R.; Teat, S. J. *Acta Crystallogr.* **2004**, *E60*, 01226–01228.
- (48) Takahashi, S.; Kariya, M.; Yatake, T.; Sonogashira, K.; Pittman, C. U., Eds. *Organometallic Polymers*; Academic Press: New York, 1978.
- (49) Sheldrick, G. M. In *SHELXL-97, a program for crystal structure refinement*; Göttingen, Germany, 1997.
- (50) Odian, G. *Principles of Polymerization*, 3rd ed.; John Wiley & Sons: New York, 1991.
- (51) Khan, M. S.; Al-Mandhary, M. R. A.; Al-Suti, M. K.; Raithby, P. R.; Ahrens, B.; Male, L.; Friend, R. H.; Köhler, A.; Wilson, J. *J. Chem. Soc., Dalton Trans.* **2003**, 65–73.
- (52) Khan, M. S.; Al-Mandhary, M. R. A.; Al-Suti, M. K.; Feeder, N.; Nahar, S.; Köhler, A.; Friend, R. H.; Wilson, P. J.; Raithby, P. R. *J. Chem. Soc., Dalton Trans.* **2002**, 2441.
- (53) Khan, M. S.; Al-Mandhary, M. R. A.; Al-Suti, M. K.; Al-Battashi, F. R.; Al-Saadi, S.; Ahrens, B.; Bjernemose, J. K.; Mahon, M. F.; Raithby, P. R.; Younus, M.; Chawdhury, N.; Kohler, A.; Marsaglia, E. A.; Tedesco, E.; Feeder, N.; Teat, S. J. *J. Chem. Soc., Dalton Trans.* **2004**, 2377–2385.
- (54) Beljonne, D.; Cornil, J.; Friend, R. H.; Janssen, R. A. J.; Brédas, J. L. *J. Am. Chem. Soc.* **1996**, *118*, 6453–6461.
- (55) Cornil, J.; Beljonne, D.; Santos, D. A. d.; Shuai, Z.; Bredas, J. L. *Synth. Met.* **1996**, *78*, 209.
- (56) Greenham, N. C.; Ginger, D. S. *Phys. Rev. B* **1999**, *59*, 10622.
- (57) Chawdhury, N.; Köhler, A.; Friend, R. H.; Younus, M.; Long, N. J.; Raithby, P. R.; Lewis, J. *Macromol.* **1998**, *31*, 722–727.
- (58) Wittmann, H. F. Ph.D. Thesis, University of Cambridge, **1994**.
- (59) Wasserberg, D.; Marsal, P.; Meskers, S. C. J.; Janssen, R. A. J.; Beljonne, D. *J. Phys. Chem. B* **2005**, *109*, 4410.
- (60) Beljonne, D.; Cornil, J.; Bredas, J. L.; Friend, R. H. *Synth. Met.* **1996**, *76*, 61.
- (61) Turro, N. *Modern Molecular Photochemistry*; University Science: Mill Valley, CA, 1991.
- (62) Sirringhaus, H.; Brown, P. J.; Friend, R. H.; Nielsen, M. M.; Bechgaard, K.; Langeveld-Voss, B. M. W.; Spiering, A. J. H.; Janssen, R. A. J.; Meijer, E. W.; Herwig, P.; de Leeuw, D. M. *Nature* **1999**, *401*, 685–688.
- (63) Zen, A.; Saphiannikova, M.; Neher, D.; Grenzer, J.; Grigorian, S.; Pietsch, U.; Asawapirom, U.; Janietz, S.; Scherf, U.; Lieberwirth, I.; Wegner, G. *Macromolecules* **2006**, *39*, 2162–2171.
- (64) Clark, J.; Silva, C.; Friend, R. H.; Spano, F. C. *Phys. Rev. Lett.* **2007**, *98*.
- (65) Chang, J. F.; Sun, B. Q.; Breiby, D. W.; Nielsen, M. M.; Solling, T. I.; Giles, M.; McCulloch, I.; Sirringhaus, H. *Chem. Mater.* **2004**, *16*, 4772–4776.
- (66) Zen, A.; Pflaum, J.; Hirschmann, S.; Zhuang, W.; Jaiser, F.; Asawapirom, U.; Rabe, J. P.; Scherf, U.; Neher, D. *Adv. Funct. Mater.* **2004**, *14*, 757–764.
- (67) Chawdhury, N.; Köhler, A.; Friend, R. H.; Younus, M.; Long, N. J.; Raithby, P. R.; Lewis, J. *Macromolecules* **1998**, *31*, 722–727.

MA802399A